Social Cognitive and Affective Neuroscience, 2016, 1440–1448

doi: 10.1093/scan/nsw054
Advance Access Publication Date: 5 June 2016
Original article

Task-irrelevant fear enhances amygdala-FFG inhibition and decreases subsequent face processing

Barbara Schulte Holthausen[1,2], Ute Habel[1,2], Thilo Kellermann[1,2], Patrick D. Schelenz[1], Frank Schneider[1,2], J. Christopher Edgar[3], Bruce I. Turetsky[4], and Christina Regenbogen[1,2,5]

[1]Department of Psychiatry, Psychotherapy and Psychosomatics, Medical Faculty, RWTH Aachen, Aachen 52074, Germany, [2]JARA - BRAIN Institute 1: Structure Function Relationship, Jülich 52428, Germany, [3]Department of Radiology, The Children's Hospital of Philadelphia, Philadelphia, PA 19104, USA, [4]Department of Psychiatry, University of Pennsylvania, Philadelphia, PA 19104, USA, and [5]Department of Clinical Neuroscience, Karolinska Institutet, Stockholm 17177, Sweden,

Correspondence should be addressed to Barbara Schulte Holthausen, Department of Psychiatry, Psychotherapy and Psychosomatics, Medical Faculty, RWTH Aachen, Pauwelsstraße 30, D-52074 Aachen, Germany. E-mail: baschulte@ukaachen.de.

Abstract

Facial threat is associated with changes in limbic activity as well as modifications in the cortical face-related N170. It remains unclear if task-irrelevant threat modulates the response to a subsequent facial stimulus, and whether the amygdala's role in early threat perception is independent and direct, or modulatory. In 19 healthy participants, crowds of emotional faces were followed by target faces and a rating task while simultaneous EEG-fMRI data were recorded. In addition to conventional analyses, fMRI-informed EEG analyses and fMRI dynamic causal modeling (DCM) were performed. Fearful facial crowds reduced EEG N170 target face amplitudes and increased responses in a fMRI network comprising insula, amygdala and inferior frontal cortex. Multimodal analyses showed that amygdala response was present ~60 ms before the right fusiform gyrus-derived N170. DCM indicated inhibitory connections from amygdala to fusiform gyrus, strengthened when fearful crowds preceded a target face. Results demonstrated the suppressing influence of task-irrelevant fearful crowds on subsequent face processing. The amygdala may be sensitive to task-irrelevant fearful crowds and subsequently strengthen its inhibitory influence on face-responsive fusiform N170 generators. This provides spatiotemporal evidence for a feedback mechanism of the amygdala by narrowing attention in order to focus on potential threats.

Key words: amygdala, EEG-fMRI, faces, priming, threat processing

Introduction

Emotional face processing is an universal and adaptive process that facilitates verbal and non-verbal communication as well as the evaluation of potential threats (Dolan, 2002; Ekman and Friesen, 1971). Fearful and angry facial expressions signal potential danger, and rapid threat decoding is hypothesized to provide a survival benefit even when the nature of the threat is not fully evaluated (Adolphs, 2008). On a behavioral level, this 'threat-priority' processing results in faster reaction times and increased detection performance (Hansen and Hansen, 1988; Eastwood *et al.*, 2001; Öhman *et al.*, 2001; but see Purcell and Stewart, 2010; Savage *et al.*, 2013).

Perceiving and detecting an emotional expression is associated with amygdala blood oxygenation level dependent (BOLD) changes, with strong evidence for the amygdala's involvement in fearful stimulus processing (Davis, 1992; LeDoux, 2003). More precisely, the amygdala is hypothesized to modify visual encoding of salient social information (Morris *et al.*, 1996; Furl *et al.*,

Received: 23 October 2015; **Revised:** 18 March 2016; **Accepted:** 18 April 2016

2013), even when outside of the attentional focus (Vuilleumier *et al.*, 2001; Öhman, 2005). The amygdala is further interconnected with visual areas, and disruption to these pathways results in impaired perception and recognition of emotional facial expressions (Adolphs *et al.*, 1994). Its clinical relevance is evident in several psychiatric conditions; e.g. trait anxiety and depression are associated with hyperactivity of the amygdala (Sheline *et al.*, 2001; Bishop *et al.*, 2007).

Intracranial findings indicate amygdala involvement soon after stimulus presentation, up to 100 ms before higher-order saliency evaluation and action preparation analyses in areas such as the insular cortex (Krolak-Salmon *et al.*, 2004; Menon and Uddin, 2010). Contemporary models focus on the amygdala's exact contribution in threat perception. Models in favor of a so-called 'low road' approach hypothesize that the amygdala is directly involved in the automatic processing of affective information via a rapid subcortical pathway that bypasses primary cortical areas (Garrido *et al.*, 2012; Garvert *et al.*, 2014). Other models assume that the amygdala acts modulatory via connections with primary visual and prefrontal areas, thus highlighting the amygdala's function in coordinating cortical networks during danger and threat evaluation (Morris *et al.*, 1998; Pessoa and Adolphs, 2010). Studies examining the above have focused on automatic threat processing and the results have increased our understanding of the basic mechanisms. (Whalen *et al.*, 1998; Liddell *et al.*, 2005; Williams *et al.*, 2006). However, in real life, potential dangers are not isolated from their surroundings.

Contextual factors such as scenes, voices, or even other faces influence identification accuracy and reaction times, as well as the perceived intensity levels of target faces (Masuda *et al.*, 2008; Righart and de Gelder, 2008b; Aviezer *et al.*, 2011). On a neural level, context information is processed at an early perceptual stage (N170), with joint activation in temporal and occipital brain regions (Righart and de Gelder, 2006, 2008a) as well as in prefrontal regions (Lee and Siegle, 2014). This suggests that context has an effect on early markers of visual perception via rapid recruitment of a wide cortical network. It remains unclear how fearful context influences the subsequent processing of a target face and how the amygdala contributes to early threat processing.

The present study examined the impact of an emotional task-irrelevant facial crowd on behavioral and neural parameters of a subsequently-presented target face. Obtaining simultaneous EEG-fMRI, the present study sought to delineate when and where in the brain an emotional crowd influences target face processing, focusing on the N170 event-related potential (ERP). The N170 is associated with early face processing and assumed to be generated by the fusiform face gyrus (FFG, Herrmann *et al.*, 2005; Deffke *et al.*, 2007). Whereas some studies speak in favor of an emotion sensitivity of the N170 (Blau *et al.*, 2007), others found the N170 to be emotion-unspecific (Eimer and Holmes, 2002; Herrmann *et al.*, 2002). To examine the above issues, crowd and target-face N170 amplitudes and latencies as well as BOLD-activation changes of target faces were analyzed. We hypothesized that (i) task-irrelevant fearful facial crowds would decrease target identification, intensity ratings and increase reaction times as well as (ii) modulate the N170 amplitude to target faces and that (iii) targets preceded by fearful facial crowds would be associated with BOLD-responses in a visual-limbic network that includes the amygdala.

Methods

The experiment conformed to the Code of Ethics of the World Medical Association and was approved by the local Institutional Review Board. Participants gave written informed consent and were reimbursed 40 Euro.

Participants

Twenty-four participants (12 females) were recruited by means of local advertisements and were screened to confirm a negative life-time history of psychiatric or neurological disorders, or current substance abuse (SKID light, Wittchen, 1997). Participants were right-handed (Oldfield, 1971), had normal or corrected-to-normal vision, and fulfilled MR-scanning criteria.

After excluding three participants due to gross movement artifacts in the MR data and two participants due to EEG artifacts, the final sample comprised of 19 participants (10 females) with an average age of $M = 33.68$ years ($SD = 11.2$).

Stimuli and task

Stimuli consisted of a circularly shaped crowd of six faces ('crowd', half females) all expressing the same emotion (happy, neutral or fearful). Crowds of scrambled faces were prepared with a mosaic filter in Adobe® Photoshop® 6.0 and represented a control condition. The crowds defined the four experimental conditions ('happy', 'neutral', 'fearful', 'scrambled' [crowd]). In the center of each facial crowd, target faces of different emotions (happy, neutral, fearful) were shown ('targets').

All pictures were taken from a standardized stimulus set (Gur *et al.*, 2002), with final stimuli comparable regarding age, emotion valence and intensity. Targets were displayed in the center of the screen, with the crowd arranged circle-wise around the target face having a diameter of 11.73 cm (12.7°). The crowd-target distance (midpoint to midpoint) was 6.4° visual angle (Fox *et al.*, 2000; Adamo *et al.*, 2010a,b). The sex ratio of target and crowd faces was balanced. Images were adjusted in size (3.6 × 5.8 cm, 3.9° × 6.26° visual angle) and presented on a grey background.

Each crowd condition consisted of 120 trials (each stimulus shown twice), resulting in a total of 480 trials. Conditions were presented in pseudo-randomized order. A trial consisted of a visually presented facial crowd with a fixation cross in the center, signaling the position of the subsequently presented target and supporting gaze fixation (Figure 1). After 300 ms, a target face replaced the fixation cross and the crowd-target combination was presented for 500 ms. The stimulus presentation was followed by a blank screen (450 ms) which was incorporated to avoid an overlap of response-related movement with the signal of interest. Following this, a response screen was shown for 3500 ms. Participants were asked to identify the target emotion on a seven-point scale ranging from extremely fearful through neutral (middle icon) to extremely happy. Final decisions had to be made within 3500 ms. Half of the participants were presented with the reversed scale (extremely happy on the left side and extremely fearful on the right). A jittered fixation cross was shown for a mean duration of 875 ms before the next trial.

The experiment was divided into four parts of 120 trials each. Stimuli were presented via MR-compatible goggles using Presentation® (version 14, Neurobehavioral Systems Inc., San Francisco, CA), and button presses were recorded via an MR-compatible response system (LUMItouch^{TM}, Lightwave Technologies, Canada). Participants completed practice trials outside the scanner using faces from the same stimulus set,

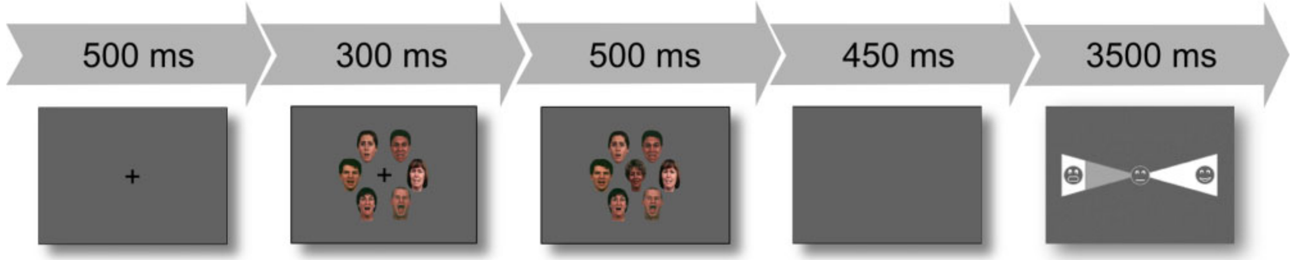

Fig. 1. Experimental design set-up.

although displaying faces different from those used in the main experiment.

Procedure

EEG sensor positions were digitized using a 3D localization device (Zebris Medical GmbH, Germany). MR-compatible EEG-caps (Easycap GmbH, Germany) with 64 Ag-AgCl electrodes (10–20 system) were used, with an additional ECG electrode placed under the left collar bone. AFz and FCz served as the recording reference and ground channel, respectively. Impedance levels were below 10 KΩ (except ECG).

Participants were placed in the 3 Tesla MR scanner (Siemens TimTrio®, Siemens Medical Systems, Germany) with their fingers positioned on the response buttons. The EEG cap was connected to an MR-compatible amplifier system (two BrainAmp MR plus 32-channel amplifiers, Brain Products GmbH, Germany) and a sync box (Brain Products) was used for synchronization of EEG recordings with the MRI slice acquisition clock. EEG data were recorded in BrainVision Recorder software (v 1.05, Brain Products) at a 5000 Hz sampling rate (0.01–250 Hz analog band-pass filter).

Functional MRI data were obtained during four runs with an echo-planar imaging (EPI) T2* contrast sequence sensitive to blood oxygenation level dependent (BOLD) changes (TR/TE = 2000/30 ms, 76° flip angle, 3.125*3.125*3.4 mm^3 voxel size, 64*64 matrix, 200*200 mm^2 FOV, 33 3.4 mm-thick axial AC-PC slices with 0.51 mm gap, recorded in ascending sequential slice acquisition) with whole brain coverage using a 12-channel head coil.

Following the fMRI task, a high-resolution whole-brain anatomical image was acquired (MPRAGE, T1-weighted, TR/TE = 1900/2.52 ms; 9° flip angle, 1 mm isotropic voxels, 256*256 matrix, 250*250 mm^2 FOV, 176 sagittal slices).

Data analysis

Behaviour

Each participant's hit rate responses (correctly identified target face emotions) were 2arcsin-transformed to transfer binomial data into a normal distribution. Reactions <150 ms were discarded (1.3%). For each outcome variable (correctly identified targets, mean intensity ratings, duration until first button press) a repeated measurement general linear model (GLM) was calculated using the within-subject factor 'crowd emotion' (four levels) with IBM® SPSS® (version 20). The GLM analyzing mean intensity ratings included fewer trials due to exclusion of neutral target faces.

EEG

Offline EEG data analysis was accomplished using BrainVision Analyzer software (version 2.0, Brain Products). Continuous EEG data underwent gradient artifact removal correction using the default procedure of the template matching algorithm in BrainVision Analyzer (Allen *et al.*, 2000). The data were low-pass-filtered with an infinite impulse response filter (IIR, 70 Hz, 48 dB slope) and down-sampled to 500 Hz. Cardiac pulse-correction was based on an automatically detected pulse template in the ECG channel (Allen *et al.*, 1998). R-peak markers were set at highly correlated (correlation coefficient $r = 0.7$) time points with above-threshold amplitudes (0.4–1.4) and individually inspected before template subtraction. Data were then further down-sampled to 250 Hz.

An independent component analysis (ICA, biased infomax, ECG electrode excluded; Makeig *et al.*, 1997) was conducted and components reflecting lateral or horizontal eye-movement and blink artifacts were visually identified and rejected based on topography and time course (max. three components/person). EEG data were then re-referenced to average reference and pseudo-electrodes AFz and FCz were spherically interpolated before final filtering was applied (IIR, 0.5-30 Hz, 24 dB slope).

Continuous EEG data were segmented into −500 to 300 ms epochs around the target stimuli. Epochs were baseline corrected from −50 to 50 ms (Eimer *et al.*, 2010). For the N170, ERP grand averages (GAVG) for each condition were computed (i.e. across subjects). Subject-specific N170 amplitudes (peak ± 20 ms) and latencies were extracted within a 40 ms search window centered on the condition-specific GAVG N170 latencies (local minimum between 160 and 200 ms) at electrodes P7 and P8 (Calder *et al.*, 2011). This yielded four target stimulus amplitude areas and latencies per participant and electrode. Additionally, we compared crowd latencies and amplitudes (epoch: −200 to 300 ms, baseline correction: −200 to 0 ms). Target- and crowd-N170 amplitudes and latencies were each analyzed with separate GLMs. The models each included the factors 'crowd emotion' (happy, neutral, fearful, scrambled) and 'electrode position' (P7 and P8). Post-hoc paired *t*-tests were Bonferroni-corrected.

fMRI

Data analysis was performed using SPM8 (Wellcome Department of Cognitive Neurology, UK). The first three functional volumes were discarded. Data preprocessing included realignment to correct for head movement and co-registration of the anatomical scan to the mean functional image. The anatomical scan was segmented to obtain parameters for a spatial transformation into the Montreal Neurologic Institute (MNI) image space (Ashburner and Friston, 2005). These normalization parameters were applied to the whole time-series and images were resampled to a voxel size of 1.5 mm^3 and smoothed with

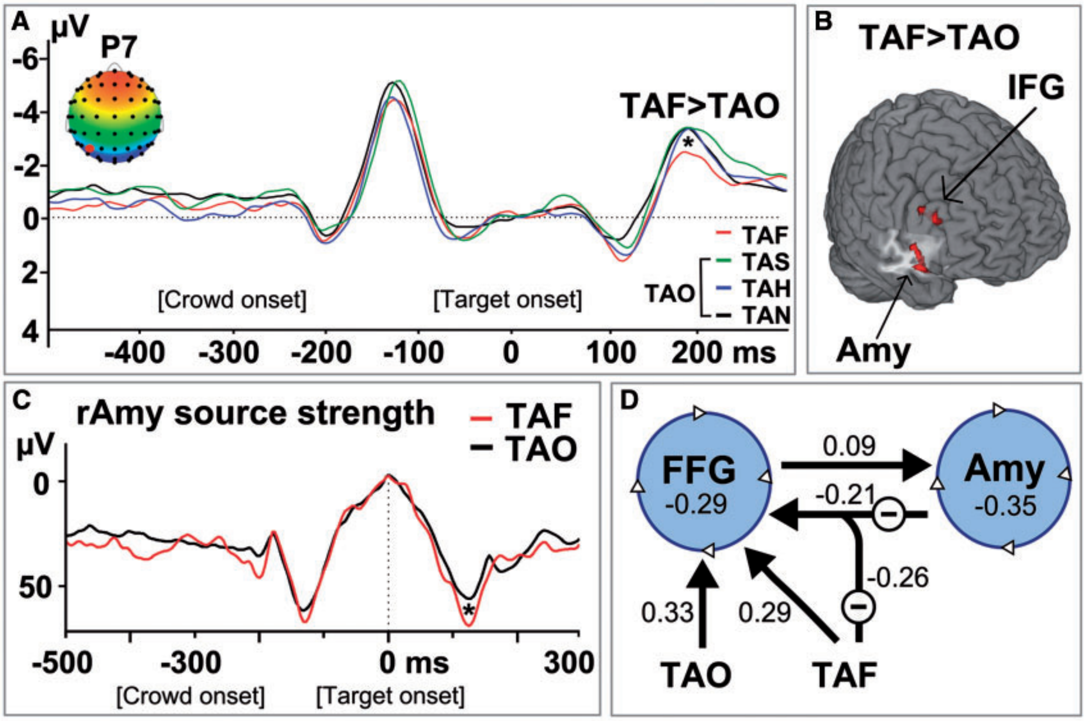

Fig. 2. A summary of the main results showing (A) ERP waveform of target N170 at P7, (B) significant fMRI clusters of the contrast 'targets preceded by fearful crowds (TAF)' > 'targets preceded by all other crowds (TAO)', ($T > 3.207$, MC-cluster-level corrected, $P < 0.05$), (C) source waveform differences in the right amygdala comparing TAF and TAO with a focus on the time-point around 124 ms, (D) the winning DCM model with corresponding coupling parameters.

an isotropic 8 mm FWHM (full width at half maximum) Gaussian kernel.

For each subject, four regressors modeled all correctly answered target onsets within one crowd condition, a separate regressor included all incorrect trials by convolving the respective stick-function with the canonical double-gamma hemodynamic response function (HRF). Realignment parameters were included as covariates of no interest. A 128 s high-pass filter was applied and serial auto-correlations were accounted for by including a first order autoregressive model.

Four T-contrasts were created, each testing for the main effect of all stimuli shown after a specific crowd emotion [targets after fearful crowd (TAF), after happy (TAH), after neutral (TAN) or after scrambled crowds (TAS)], respectively, which were further used for the group-level analysis. A mixed-effects GLM was used for group-level inference with subjects included as random effects and crowd emotion included as fixed effects. Deviations from sphericity were corrected for by variance components for within-subjects measures and heteroscedasticity between subjects and conditions.

In order to test for differences between targets after fearful crowds (TAF) compared to all other conditions, a T-test was carried out, comparing TAF to targets preceded by any other crowds (TAO, average of TAH, TAN and TAS). To estimate the overall significance level for thresholding fMRI data the AFNI AlphaSim toolbox (Cox, 1996) was used, using a gray-matter mask to limit the number of voxels. AlphaSim simulations provided a *t*-value ($T = 3.207$, $P = 0.001$ uncorrected) and cluster size (122 voxels) combination that corresponded to a familywise error rate threshold of .05 within a cluster. Group-level statistical parametric maps were anatomically categorized using the Anatomy Toolbox (Eickhoff *et al.*, 2005).

fMRI-informed EEG

A source model, with sources placed according to the peak coordinates of the group-level fMRI main findings, modeled the temporal course of neural activity using BESA MRI® and BESA Research® 5.3 software (BESA, Germany). For each participant, co-registration of EEG and MRI data was accomplished using a least-square fit of digitized head surface points (including digitized electrode positions) to the participant's anatomical scan. The individual's ERP average for the two conditions of interest—TAF ('targets after fearful crowd') and TAO ('target after any other crowd') —were imported into BESA. A standard source model was obtained by placing five regional sources at the center of mass coordinates identified from the group-level fMRI results (Table 2, Silton *et al.*, 2010; Silton *et al.*, 2011). Given the visual and fusiform activity present during emotional face recognition tasks (Haxby *et al.*, 2000) and this activity is likely removed in fMRI via the contrasts, regional sources in right and left fusiform gyri and in right and left primary visual cortex (BA 17) were also added. The locations of the primary and face-sensitive sources were thus obtained from the peak maximum (left/right) of primary visual activation in the average contrast over all four conditions (FFGr [33 -46 -17], FFGl [-33 -46 -17], BA17r [13 -82 4], BA17l [-13 -82 4] MNI [mm]). This standard source model was applied to each participant's averaged ERP data. The associated source waveforms were baseline-corrected (-50/50 ms) around the target presentation. According to the study's hypotheses, analyses were restricted to a comparison of TAF versus TAO waveforms across all participants. Based on visual inspection (see Figure 2C), peak source strength at two time periods was extracted: 124 ± 8 ms and 188 ± 8 ms. Mean source strength was compared using paired T-tests in SPSS®.

Table 1. Grand-average ERP waveforms of crowd- and target-face N170 amplitude area (± 20 ms) and latency for each condition reported for electrode positions P7 and P8

	Crowd N170				Target N170			
	Amplitude (SD)		Latency (SD)		Amplitude (SD)		Latency (SD)	
Crowd emotion	P7	P8	P7	P8	P7	P8	P7	P8
Fearful	−5 (3.2)	−4.2 (3.1)	175 (12)	176 (11)	**−3.4 (4)**	**−2.7 (2.4)**	188 (11)	191 (14)
Happy	−4.5 (3.5)	−4.4 (3.8)	175 (9)	173 (11)	−4.8 (3.8)	−4.1 (2.4)	192 (13)	195 (12)
Neutral	−3.9 (3.3)	−4 (3.3)	172 (12)	173 (11)	−5 (3.7)	−4.7 (3)	188 (13)	183 (11)
Scrambled	−4.4 (3.4)	−4.3 (3.4)	**183 (8)**	**181 (12)**	−5 (3.1)	−3.6 (2.3)	195 (12)	195 (12)

Numbers printed in bold depict significant differences between the respective condition and all other conditions.

Results

Behavior

Participants identified $M = 87.35\%$ ($SD = 0.046$) of target stimuli correctly. Separate GLMs for repeated measurements analyzing the effect of 'crowd emotion' on hit rates (P=.767), intensity ratings (P=.418), or first response (P=.362) showed no significant effects. This showed that 'crowd emotion' did not differentially affect accuracy, intensity ratings or duration until first button press.

EEG

N170 of crowd faces

Amplitude: A GLM for repeated measurements analyzing the influence of 'crowd emotion' and 'electrode position' as well as their interaction on crowd N170 amplitudes did not yield any significant effects.

Latency: The GLM analysis (repeated measures, same factors as for the amplitude analysis) revealed a significant main effect of 'crowd emotion' on crowd N170 latencies ($F_{(3,1)}$=14.727, p<0.001, η^2 = 0.45). Post-hoc comparisons showed that the scrambled crowd N170 peaked significantly later than the crowd N170 responses to stimuli depicting human faces (scrambled compared to fearful $t_{(18)} = 4.34$, to happy $t_{(18)} = 4.68$, and to neutral crowds $t_{(18)} = 5.89$, all $ps < 0.001$, see Table 1 for mean values and standard deviations of crowd and target N170 amplitudes and latencies at P7 and P8). No significant effect was found for 'electrode position' or for the interaction of 'electrode position' and 'crowd emotion'.

Summarized, analyses on crowd N170 amplitudes and latencies showed that neither crowd emotion nor electrode position affected the crowd N170 amplitude. Further, a scrambled crowd led to a longer crowd N170 latency compared to facial crowds (happy, fearful, neutral).

N170 of target faces following crowds

Amplitude: The GLM analysis (repeated measures, factors 'crowd emotion' and 'electrode position') yielded a main effect of 'crowd emotion' ($F_{(3,1)} = 11.644$, $P < 0.001$, $\eta^2 = 0.393$) on target N170 amplitudes (Figure 2A). Post-hoc comparisons showed that targets preceded by fearful crowds had a reduced N170 amplitude compared to all other conditions (fearful compared to happy $t_{(18)} = 5.15$, $P < 0.001$, to neutral $t_{(18)} = 4.71$ $P < 0.001$, and to scrambled crowds $t_{(18)} = 2.99$, $P = 0.008$). No significant effect was found for 'electrode position' or the interaction of 'electrode position' and 'crowd emotion'. A follow-up GLM analysis (repeated measures) explicitly testing whether the N170 amplitude reduction in target faces (happy, neutral, and fearful) preceded by fearful crowds would be differently affected was not significant ($F_{(1.53,1)} = 0.325$, $P = 0.668$).

Table 2. Significant fMRI clusters of the T-contrast 'targets after fearful crowd TAF' > 'targets after all other crowds TAO', ($T > 3.207$, MC cluster level-corrected, $P < 0.001$)

Brain region	Hemisphere	Size	T	x	y	z
Insula	L	210	4.78	−38	18	−1
Supplementary motor area (SMA)	R	351	4.64	8	−12	60
Superior temporal gyrus (STG)	R	153	4.63	53	−33	4
Inferior frontal gyrus (IFG)	R	208	4.45	47	29	22
Amygdala	R	259	4.34	36	5	−26

Stereotaxic coordinates of local maxima of significant clusters are expressed as x;y;z values in MNI space.

Latency: A GLM (repeated measures, same factors as for the amplitude analysis) yielded a main effect 'crowd emotion' on target N170 latencies ($F_{(3,1)} = 6.017$, $P = 0.001$, $\eta^2 = 0.251$). Post-hoc comparisons revealed that targets preceded by a neutral crowd had a shorter N170 latency than targets preceded by scrambled ($t_{(18)} = -3.34$, $P = 0.004$) or happy crowds ($t_{(18)} = -4.3$, $P < 0.001$), but not by fearful crowds ($t_{(18)} = -1.64$, $P = 0.119$). Similarly, targets preceded by fearful crowds had shorter N170 latencies than targets after scrambled crowds ($t_{(18)} = -2.78$, $P = 0.012$), and trendwise shorter than targets after happy crowds ($t_{(18)} = -1.66$, $P = 0.114$). Latency differences of the crowd N170 and the target N170 were also compared to determine if differences in target N170 latencies might be due to a latency shift present in the crowd N170. Differences between crowd and target N170 latencies did not differ between the four conditions ($F_{(2.32,1)} = 2.473$, $P = 0.089$). No significant effects were found for 'electrode position' or the interaction of 'electrode position' and 'crowd emotion' on target N170 latency.

Summarized, analyses on target N170 amplitude and latency revealed that fearful crowds reduced target N170 amplitudes, independent of the emotion of the target. Further, neutral and fearful crowds were followed by shorter target N170 latencies compared to target N170 latencies preceded by happy and scrambled crowds.

fMRI group-level GLM

The T-contrast ('TAF'>'TAO') was thresholded at an alpha level of $P < 0.001$ (MC-cluster-corrected, $P < 0.05$). This contrast resulted in five significant clusters: left insula, right supplementary motor area (SMA), right superior temporal gyrus (STG), right inferior frontal gyrus (IFG) and right amygdala (Table 2, Figure 2B).

Table 3. Grand-average target source waveforms in the five regions of the fMRI-contrast (Table 2) and four additional visual sources, comparing 'targets after fearful crowds TAF' to 'targets after all other crowds TAO' and resulting *P* values of early and late peak area (± 8 ms) comparisons

Brain region	Early peak amplitude (124 ms) (SD)			Late peak amplitude (188 ms) (SD)		
	Fearful crowd	All other crowds	P	Fearful crowd	All other crowds	P
Insula l	49.6 (27.5)	41.5 (21.9)	0.166	41.3 (50)	54.9 (46.3)	0.051
SMA r	23.6 (14)	19.8 (10.1)	0.143	**19.9 (20.3)**	**29.4 (19)**	**0.008**
STG r	32.2 (17.5)	32 (22.7)	0.957	23.8 (20.6)	28.2 (16)	0.177
IFG r	**26.6 (17)**	**19.3 (14)**	**0.018**	20.9 (21.7)	25.1 (18.4)	0.148
Amygdala r	**75.4 (53.3)**	**60.5 (41.2)**	**0.028**	38.3 (36.2)	43.9 (41.3)	0.388
FFG r	22.2 (22)	22.8 (25.3)	0.875	20 (20.1)	27.4 (21)	0.095
FFG l	28.6 (20)	28.9 (17.3)	0.938	**25.3 (14.2)**	**35.7 (20)**	**0.018**
A17 r	27.4 (25.9)	27.7 (21.8)	0.946	**43.5 (47.3)**	**66.2 (46.8)**	**0.008**
A17 l	34.9 (24.8)	31.1 (20.4)	0.427	**41.5 (40.2)**	**58.2 (45.4)**	**0.011**

Numbers printed in bold depict significant differences between the two conditions.

Using a less conservative threshold ($P < 0.001$, uncorrected), significant clusters in insula, SMA and IFG were also present in the respective opposite hemisphere.

fMRI-informed EEG

We further analyzed source-strength differences between TAF and TAO in all activated clusters from the contrast TAF > TAO as well as from bilateral primary visual cortices and bilateral FFG (Table 3). Multiple comparisons were not Bonferroni-corrected, given that EEG source analyses primarily only provided additional information regarding the fMRI findings (Silton *et al.*, 2010, 2011). Source-strength comparisons for the *early* window (124 ± 8 ms) showed higher values in the right IFG ($t_{(18)} = -2.596$, $P = 0.018$) and in the right amygdala ($t_{(18)} = -2.395$, $P = 0.028$) for TAF versus TAO (Figure 2C). No other waveform time periods showed significant differences. Source-strength comparisons for the *late* time window (188 ± 8 ms) showed greater source-strength of TAO versus TAF in the right SMA ($P = 0.008$), left FFG ($P = 0.018$), and in bilateral primary visual cortex ($P = 0.008$ and $P = 0.011$, respectively). A trend for greater source-strength in TAO versus TAF was evident in the insula ($P = 0.051$) as well as in the right FFG ($P = 0.095$). No other waveform time periods showed significant differences. Summarized, greater source-strength of TAF than TAO was found in the right IFG and right amygdala around 124 ms. At around 188 ms TAO exhibited greater source-strength in the right SMA, left FFG and the primary visual cortex.

DCM

A bivariate Pearson correlation analysis of N170 amplitudes and extracted data from the activated clusters in the right amygdala revealed a significant association ($r = 0.391$, $P < 0.001$), with greater amygdala activation corresponding to smaller (less negative) N170 amplitudes. This suggested an association between a fearful crowd and reduced target face processing, potentially modulated by the amygdala. This was further explored by applying a dynamic causal modeling approach on the fMRI time-series (DCM 10, Friston *et al.*, 2003), focusing on fusiform gyrus (FFG) and amygdala associations. Time-series were extracted in each individual's right amygdala and right FFG from within 5-mm spheres around the coordinates from each individual's nearest local maximum around the group-level peak coordinate (amygdala [36 5 −26], FFG [33 −46 −17] MNI [mm]). Time-series were corrected for low-frequency drifts and effects of no interest.

The model consisted of two nodes (FFG, amygdala) with reciprocal connections. Bayesian model selection (BMS) was performed on a small model space consisting of four models using fixed effects. The FFG served as the input region for visual information of the two conditions 'TAF' and 'TAO' in all models (Model 1 without any further inputs). 'TAF' either formed a direct input into the amygdala (Model 2) or a modulatory input onto the connection from the amygdala to the FFG (Model 3) or both (Model 4).

Posterior probabilities provided by the BMS indicated superiority of Model 3 with a probability of 99.78%. The size of the coupling parameters was inferred using Bayesian model averaging (Penny *et al.*, 2010) and exhibited an inhibitory connection from the amygdala to the FFG which was further reduced (inhibited) by a modulatory input of targets preceded by fearful crowds (Figure 2D).

Taken together, dynamic causal modeling suggested a model with an increased inhibition of the amygdala onto the FFG when targets were preceded by fearful crowds.

Discussion

Task-irrelevant facial crowds influence subsequent target face processing, despite being outside of the focus of attention. Robust evidence supporting this was obtained from both functional imaging and electrophysiological perspectives. N170 latencies of scrambled crowds were significantly delayed, relative to the N170 latencies of facial crowds. Together with previous findings, such as the N170 latency increase for inverted and ape faces (compared to upward and human faces, respectively), this confirms humans' selective sensitivity to faces (Itier and Taylor, 2004; Rousselet *et al.*, 2004). Apart from this general effect, the data demonstrated that specifically *fearful* facial crowds have prolonged perceptual consequences. Fearful and neutral crowds were both followed by shorter target N170 latencies. Since neutral faces are, at times, perceived as emotionally ambiguous (Cooper and Langton, 2006; Santesso *et al.*, 2008), this suggests that potentially threatening crowds induce a quick scan of the environment to identify possible dangers. Also, fearful facial crowds reduced target N170 amplitudes, while the N170 amplitude of the crowd itself was unaffected. Crowd stimuli signaling danger or threat thus reduced neural activity associated with a subsequently presented face, irrespective of whether or not the target face itself signaled danger or threat. Of note, behavioral parameters (emotion recognition accuracy, intensity ratings, and time until first button press) were not sensitive to the presentation of fearful facial crowds. This may reflect the use of a delayed button press response following target presentation. To address this limitation, we have recently conducted a behavioral follow-up study (Schulte Holthausen *et al.*, 2016; $N = 29$, 14 females, mean age 26.1 years, $SD = 5.37$). The study applied the same experimental design but incorporated an immediate post-stimulus response (i.e. no 450 ms delay). Here, target faces preceded by fearful crowds were associated with decreased emotion recognition accuracy ($t_{(28)}=2.176$, $P = 0.038$) and increased reaction times ($t_{(28)} = 1.976$, $P = 0.058$). Together with the main study, these findings indicate that threat causes earlier but smaller target N170 amplitudes and also decreases emotion recognition accuracy and speed.

Whereas an initial broad scan with faster stimulus perception (target N170 latency) may be beneficial for threat detection, such scanning seems to be associated with more superficial processing (smaller target N170 amplitude) and further potential attention restriction. The latter is confirmed by the slower and less accurate behavioral responses, suggesting that there is a time window in which the capacity for evaluating subsequent stimuli is limited.

The present findings extend the notion of unconscious and automatic threat processing (Whalen et al., 1998; Williams *et al.*, 2006) to a situation where participants focused only on target faces and 'ignored' presented crowd faces. The corresponding BOLD-activations of this 'threatening after-effect' (TAF > TAO) were located in a corticolimbic network of bilateral insula, SMA, IFG and unilateral STG, as well as right amygdala. The amygdala is not only involved in emotion processing, valence evaluation and saliency detection per se (Anderson and Phelps, 2001; Todorov and Engell, 2008), but also in early threat perception and evaluation (Morris *et al.*, 1996; Haxby *et al.*, 2002; Furl *et al.*, 2013). The early perception and evaluation of fearful faces by the amygdala and anterior insula likely facilitates appropriate behavioral responses to danger detection. These include sensorimotor responses coordinated by a network of OFC, cingulate cortex and brainstem (Morris *et al.*, 1998). The clusters in the IFG and STG are thought to be part of this early fear detection and evaluation network. To further understand the role of the amygdala, a fMRI-informed EEG source analysis was carried out and revealed the presence of stronger early amygdala and IFG involvement approximately 120 ms after fearful crowd presentation, and a reduction of source activity in areas of the face-processing network after 180 ms. This motivated follow-up source dynamic analyses to investigate whether the amygdala activation difference between TAF and TAO was causally related to the reduced target N170 amplitudes. A DCM tested whether the 'threatening-after-effect' would indicate a direct 'low road' pathway into the amygdala, or a modulatory input onto the amygdala-FFG connection. Bayesian model selection confirmed the modulatory input model with high confidence. Specifically, TAF increased amygdala inhibition of the FFG, indicating a modulatory and attention-allocating role of the amygdala when processing threat-signaling stimuli.

To conclude, present results extend findings regarding the relationship between amygdala and face processing areas in threat perception and evaluation (Morris *et al.*, 1998; Pessoa and Adolphs, 2010; Herrington *et al.*, 2011) to the situation of perceiving a facial stimulus *preceded* by threat. In particular, task-irrelevant yet salient fearful facial crowds cause an inhibitory impact of the amygdala on fusiform face-processing areas. Hence, the combination of temporal and spatial data suggest that the amygdala is not independently involved in threat processing by bypassing cortical regions ('low road') through a subcortical pathway. Rather, the role of the amygdala appears to be modulatory through connections to primary visual and face-processing areas. Stronger inhibition of face processing areas when fearful facial crowds precede a target face suggests a feedback mechanism by which the amygdala efficiently coordinates cortical networks during threat evaluation. A faster but more superficial first scan is then followed by a potential attention restriction, which might be modulated by the amygdala. While futures studies should investigate later occurring ERP components reflecting attention allocation to disentangle the complex effect of threat-related stimuli on subsequent faces in more detail, it can be concluded that re-focusing of attention may be a beneficial and adaptive strategy which provides an increased focus on potential threats.

Funding

This work was supported by the International Research Training Group (IRTG 1328) of the German Research Foundation (DFG) and by the Brain Imaging Facility of the Interdisciplinary Center for Clinical Research within the Faculty of Medicine at the RWTH Aachen University. CR was supported by a postdoctoral fellowship from the DAAD. TK was supported by the START Program of the Faculty of Medicine, RWTH Aachen University (START 135/14).

Conflict of interest. None declared.

References

Adamo, M., Pun, C., Ferber, S. (2010a). Multiple attentional control settings influence late attentional selection but do not provide an early attentional filter. *Cognitive Neuroscience*, **1**, 102–10.

Adamo, M., Wozny, S., Pratt, J., Ferber, S. (2010b). Parallel, independent attentional control settings for colors and shapes. *Attention, Perception, & Psychophysics*, **72**(7), 1730–5.

Adolphs, R. (2008). Fear, faces, and the human amygdala. *Current Opinion in Neurobiology*, **18**, 166–72.

Adolphs, R., Tranel, D., Damasio, H., Damasio, A. (1994). Impaired recognition of emotion in facial expressions following bilateral damage to the human amygdala. *Nature*, **372**, 669–72.

Allen, P.J., Josephs, O., Turner, R. (2000). A method for removing imaging artifact from continuous EEG recorded during functional MRI. *Neuroimage*, **12**, 230–9.

Allen, P.J., Polizzi, G., Krakow, K., Fish, D.R., Lemieux, L. (1998). Identification of EEG events in the MR scanner: the problem of pulse artifact and a method for its subtraction. *Neuroimage*, **8**, 229–39.

Anderson, A.K., Phelps, E.A. (2001). Lesions of the human amygdala impair enhanced perception of emotionally salient events. *Nature*, **411**, 305–9.

Ashburner, J., Friston, K.J. (2005). Unified segmentation. *Neuroimage*, **26**, 839–51.

Aviezer, H., Bentin, S., Dudarev, V., Hassin, R.R. (2011). The automaticity of emotional face-context integration. *Emotion*, **11**, 1406–14.

Bishop, S.J., Jenkins, R., Lawrence, A.D. (2007). Neural processing of fearful faces: effects of anxiety are gated by perceptual capacity limitations. *Cerebral Cortex*, **17**, 1595–603.

Blau, V., Maurer, U., Tottenham, N., McCandliss, B. (2007). The face-specific N170 component is modulated by emotional facial expression. *Behavioral and Brain Functions*, **3**, 7.

Calder, A., Rhodes, G., Johnson, M., Haxby, J. (2011). *Oxford Handbook of Face Perception:* Oxford: Oxford University Press.

Cooper, R.M., Langton, S.R. (2006). Attentional bias to angry faces using the dot-probe task? It depends when you look for it. *Behaviour Research and Therapy*, **44**, 1321–9.

Cox, R.W. (1996). AFNI: software for analysis and visualization of functional magnetic resonance neuroimages. *Computers and Biomedical Research*, **29**, 162–73.

Davis, M. (1992). The role of the amygdala in fear and anxiety. *Annual Review of Neuroscience*, **15**, 353–75.

Deffke, I., Sander, T., Heidenreich, J., *et al.* (2007). MEG/EEG sources of the 170-ms response to faces are co-localized in the fusiform gyrus. *NeuroImage*, **35**, 1495–501.

Dolan, R.J. (2002). Emotion, cognition, and behavior. *science*, **298**(5596), 1191–4.

Eastwood, J.D., Smilek, D., Merikle, P.M. (2001). Differential attentional guidance by unattended faces expressing positive and negative emotion. *Perception & Psychophysics*, **63**, 1004–13.

Eickhoff, S.B., Stephan, K.E., Mohlberg, H., *et al.* (2005). A new SPM toolbox for combining probabilistic cytoarchitectonic maps and functional imaging data. *Neuroimage*, **25**, 1325–35.

Eimer, M., Holmes, A. (2002). An ERP study on the time course of emotional face processing. *Neuroreport*, **13**, 427–31.

Eimer, M., Kiss, M., Nicholas, S. (2010). Response profile of the face-sensitive N170 component: a rapid adaptation study. *Cerebral Cortex*, **20**, 2442–52.

Ekman, P., Friesen, W.V. (1971). Constants across cultures in the face and emotion. *Journal of Personality and Social Psychology*, **17**, 124–9.

Fox, E., Lester, V., Russo, R., Bowles, R., Pichler, A., Dutton, K. (2000). Facial expressions of emotion: Are angry faces detected more efficiently? *Cognition & Emotion*, **14**, 61–92.

Friston, K.J., Harrison, L., Penny, W. (2003). Dynamic causal modelling. *Neuroimage*, **19**, 1273–302.

Furl, N., Henson, R.N., Friston, K.J., Calder, A.J. (2013). Top-down control of visual responses to fear by the amygdala. *Journal of Neuroscience*, **33**, 17435–43.

Garrido, M.I., Barnes, G.R., Sahani, M., Dolan, R.J. (2012). Functional evidence for a dual route to amygdala. *Current Biology*, **22**, 129–34.

Garvert, M.M., Friston, K.J., Dolan, R.J., Garrido, M.I. (2014). Subcortical amygdala pathways enable rapid face processing. *NeuroImage*, **102**, 309–16.

Gur, R.C., Sara, R., Hagendoorn, M., *et al.* (2002). A method for obtaining 3-dimensional facial expressions and its standardization for use in neurocognitive studies. *Journal of Neuroscience Methods*, **115**, 137–43.

Hansen, C.H., Hansen, R.D. (1988). Finding the face in the crowd: an anger superiority effect. *Journal of Personality and Social Psychology*, **54**, 917–24.

Haxby, J.V., Hoffman, E.A., Gobbini, M.I. (2000). The distributed human neural system for face perception. *Trends in Cognitive Sciences*, **4**, 223–33.

Haxby, J.V., Hoffman, E.A., Gobbini, M.I. (2002). Human neural systems for face recognition and social communication. *Biological Psychiatry*, **51**, 59–67.

Herrington, J.D., Taylor, J.M., Grupe, D.W., Curby, K.M., Schultz, R.T. (2011). Bidirectional communication between amygdala and fusiform gyrus during facial recognition. *Neuroimage*, **56**, 2348–55.

Herrmann, M.J., Aranda, D., Ellgring, H., *et al.* (2002). Face-specific event-related potential in humans is independent from facial expression. *International Journal of Psychophysiology*, **45**.

Herrmann, M.J., Ehlis, A.C., Muehlberger, A., Fallgatter, A.J. (2005). Source localization of early stages of face processing. *Brain Topography*, **18**, 77–85.

Itier, R.J., Taylor, M.J. (2004). Source analysis of the N170 to faces and objects. *NeuroReport*, **15**, 1261–5.

Krolak-Salmon, P., Henaff, M.A., Vighetto, A., Bertrand, O., Mauguiere, F. (2004). Early amygdala reaction to fear spreading in occipital, temporal, and frontal cortex: a depth electrode ERP study in human. *Neuron*, **42**, 665–76.

LeDoux, J. (2003). The emotional brain, fear, and the amygdala. *Cellular and Molecular Neurobiology*, **23**, 727–38.

Lee, K.H., Siegle, G.J. (2014). Different brain activity in response to emotional faces alone and augmented by contextual information. *Psychophysiology*, **51**(11), 1147–57.

Liddell, B.J., Brown, K.J., Kemp, A.H., *et al.* (2005). A direct brainstem–amygdala–cortical 'alarm'system for subliminal signals of fear. *Neuroimage*, **24**, 235–43.

Makeig, S., Jung, T.P., Bell, A.J., Ghahremani, D., Sejnowski, T.J. (1997). Blind separation of auditory event-related brain responses into independent components. *Proceedings of the National Academy of Sciences*, **94**, 10979–84.

Masuda, T., Ellsworth, P.C., Mesquita, B., Leu, J., Tanida, S., Van de Veerdonk, E. (2008). Placing the face in context: Cultural differences in the perception of facial emotion. *Journal of Personality and Social Psychology*, **94**, 365.

Menon, V., Uddin, L.Q. (2010). Saliency, switching, attention and control: a network model of insula function. *Brain Structure & Function*, **214**,655–67.

Morris, J.S., Friston, K.J., Buchel, C., *et al.* (1998). A neuromodulatory role for the human amygdala in processing emotional facial expressions. *Brain* **121**, 47–57.

Morris, J.S., Frith, C.D., Perrett, D.I., *et al.* (1996). A differential neural response in the human amygdala to fearful and happy facial expressions. *Nature*, **383**, 812–5.

Öhman, A. (2005). The role of the amygdala in human fear: automatic detection of threat. *Psychoneuroendocrinology*, **30**, 953–8.

Öhman, A., Lundqvist, D., Esteves, F. (2001). The face in the crowd revisited: A threat advantage with schematic stimuli. *Journal of Personality and Social Psychology*, **80**, 381–96.

Oldfield, R.C. (1971). The assessment and analysis of handedness: the Edinburgh inventory. *Neuropsychologia*, **9**, 97–113.

Penny, W.D., Stephan, K.E., Daunizeau, J., *et al.* (2010). Comparing Families of Dynamic Causal Models. *PLoS Computational Biology*, **6**, e1000709.

Pessoa, L., Adolphs, R. (2010). Emotion processing and the amygdala: from a'low road'to'many roads' of evaluating biological significance. *Nature Reviews Neuroscience*, **11**, 773–83.

Purcell, D.G., Stewart, A.L. (2010). Still another confounded face in the crowd. *Attention, Perception, & Psychophysics*, **72**, 2115–27.

Righart, R., de Gelder, B. (2006). Context influences early perceptual analysis of faces—an electrophysiological study. *Cerebral Cortex*, **16**, 1249–57.

Righart, R., de Gelder, B. (2008a). Rapid influence of emotional scenes on encoding of facial expressions: An ERP study. *Social Cognitive and Affective Neuroscience*, **3**(3). doi: 10.1093/scan/nsn021 19015119.

Righart, R., de Gelder, B. (2008b). Recognition of facial expressions is influenced by emotional scene gist. *Cognitive, Affective & Behavioral Neuroscience*, **8**(3), 264. doi: 10.3758/CABN.8.3.264.

Rousselet, G.A., Macé, M.J.M., Fabre-Thorpe, M. (2004). Animal and human faces in natural scenes: How specific to human faces is the N170 ERP component? *Journal of Vision*, **4**, 2.

Santesso, D.L., Meuret, A.E., Hofmann, S.G., *et al.* (2008). Electrophysiological correlates of spatial orienting towards angry faces: a source localization study. *Neuropsychologia*, **46**, 1338–48.

Savage, R.A., Lipp, O.V., Craig, B.M., Becker, S.I., Horstmann, G. (2013). In search of the emotional face: Anger versus happiness superiority in visual search. *Emotion*, **13**, 758–68.

Schulte Holthausen, B., Regenbogen, C., Turetsky, B.I., Schneider, F., Habel, U. (2016). The influence of task-irrelevant flankers depends on the composition of emotion categories. *Frontiers in Psychology*, **7**. doi: 10.3389/fpsyg.2016.00712.

Sheline, Y.I., Barch, D.M., Donnelly, J.M., Ollinger, J.M., Snyder, A.Z., Mintun, M.A. (2001). Increased amygdala response to masked emotional faces in depressed subjects resolves with antidepressant treatment: an fMRI study. *Biological Psychiatry*, **50**, 651–8.

Silton, R.L., Heller, W., Engels, A.S., *et al.* (2011). Depression and anxious apprehension distinguish frontocingulate cortical activity during top-down attentional control. *Journal of Abnormal Psychology*, **120**, 272–85.

Silton, R.L., Heller, W., Towers, D.N., *et al.* (2010). The time course of activity in dorsolateral prefrontal cortex and anterior cingulate cortex during top-down attentional control. *Neuroimage*, **50**, 1292–302.

Todorov, A., Engell, A.D. (2008). The role of the amygdala in implicit evaluation of emotionally neutral faces. *Social Cognitive and Affective Neuroscience*, doi: 10.1093/scan/nsn033.

Vuilleumier, P., Armony, J.L., Driver, J., Dolan, R.J. (2001). Effects of attention and emotion on face processing in the human brain: an event-related fMRI study. *Neuron*, **30**, 829–41.

Whalen, P.J., Rauch, S.L., Etcoff, N.L., McInerney, S.C., Lee, M.B., Jenike, M.A. (1998). Masked presentations of emotional facial expressions modulate amygdala activity without explicit knowledge. *The Journal of Neuroscience*, **18**, 411–8.

Williams, L.M., Liddell, B.J., Kemp, A.H., *et al.* (2006). Amygdala–prefrontal dissociation of subliminal and supraliminal fear. *Human Brain Mapping*, **27**, 652–61.

Wittchen, H.-U., Wunderlich, U., Gruschwitz, S., Zaudig, M. (1997). *Strukturiertes Klinisches Interview Für DSM-IV, Achse-I (SKID-I)*. Göttingen: Hogrefe.